



Providing Choice & Value

Generic CT and MRI Contrast Agents



CONTACT REP

AJNR

**Solitary Parathyroid Adenoma Localization
in Technetium Tc99m Sestamibi SPECT and
Multiphase Multidetector 4D CT**

T.H. Vu, D. Schellingerhout, N. Guha-Thakurta, J. Sun, W. Wei, S.C. Kappadth, N. Perrier, E.E. Kim, E. Rohren, H.H. Chuang and F.C. Wong

This information is current as
of July 29, 2025.

AJNR Am J Neuroradiol 2019, 40 (1) 142-149

doi: <https://doi.org/10.3174/ajnr.A5901>

<http://www.ajnr.org/content/40/1/142>

Solitary Parathyroid Adenoma Localization in Technetium Tc99m Sestamibi SPECT and Multiphase Multidetector 4D CT

T.H. Vu, D. Schellingerhout, N. Guha-Thakurta, J. Sun, W. Wei, S.C. Kappadth, N. Perrier, E.E. Kim, E. Rohren, H.H. Chuang, and F.C. Wong

ABSTRACT

BACKGROUND AND PURPOSE: Minimally invasive parathyroid surgery relies critically on image guidance, but data comparing the efficacy of various imaging modalities are scarce. Our aim was to perform a blinded comparison of the localizing capability of technetium Tc99m sestamibi SPECT, multiphase multidetector 4D CT, and the combination of these 2 modalities (technetium Tc99m sestamibi SPECT + multiphase multidetector 4D CT).

MATERIALS AND METHODS: We reviewed the records of 31 (6 men, 25 women; median age, 56 years) consecutive patients diagnosed with biochemically confirmed primary hyperparathyroidism between November 2009 and March 2010 who underwent preoperative technetium Tc99m sestamibi SPECT and multiphase multidetector 4D CT performed on the same scanner with pathologic confirmation by resection of a single parathyroid adenoma. Accuracy was determined separately for localization to the correct side and quadrant using surgical localization as the standard of reference.

RESULTS: Surgical resection identified 14 left and 17 right parathyroid adenomas and 2 left inferior, 12 left superior, 11 right inferior, and 6 right superior parathyroid adenomas. For left/right localization, technetium Tc99m sestamibi SPECT achieved an accuracy of 93.5% (29 of 31), multiphase multidetector 4D CT achieved 96.8% accuracy (30 of 31), and technetium Tc99m sestamibi SPECT + multiphase multidetector 4D CT achieved 96.8% accuracy (30 of 31). For quadrant localization, technetium Tc99m sestamibi SPECT accuracy was 67.7% (21 of 31), multiphase multidetector 4D CT accuracy was 87.1% (27 of 31), and technetium Tc99m sestamibi SPECT + multiphase multidetector 4D CT accuracy was 93.5% (29 of 31). Reader diagnostic confidence was consistently ranked lowest for technetium Tc99m sestamibi SPECT and highest for technetium Tc99m sestamibi SPECT + multiphase multidetector 4D CT.

CONCLUSIONS: For left/right localization of parathyroid adenomas, all modalities performed equivalently. For quadrant localization, technetium Tc99m sestamibi SPECT + multiphase multidetector 4D CT is superior to technetium Tc99m sestamibi SPECT.

ABBREVIATIONS: 4DCT = multiphase multidetector 4D CT; MIBI = technetium Tc99m sestamibi

Primary hyperparathyroidism is a common endocrine disorder caused most often by a solitary parathyroid adenoma.¹ The definitive cure for this disorder is surgical resection. The surgical approach has shifted from standard bilateral cervical exploration to modern minimally invasive parathyroidectomy.² For minimally invasive parathyroidectomy to be successful, accurate pre-

operative localization of a single offending parathyroid gland and exclusion of possible multigland disease or 4-gland hyperplasia are critical and useful. Several noninvasive preoperative localization modalities are available, including parathyroid scintigraphy using technetium Tc99m sestamibi (MIBI)^{3,4}; ultrasonography^{5,6}; CT, specifically multiphase multidetector 4D CT (4DCT)⁷; MR imaging⁸; and recently, ¹¹C-methionine positron-emission tomography/CT⁹ and [¹⁸F]-choline positron-emission tomography/CT.¹⁰ The emergence of hybrid SPECT camera technology and advances in CT technology have allowed MIBI SPECT and 4DCT to be successfully used for the preoperative localization of abnormal parathyroid glands.¹¹⁻¹⁶

The requirements for minimally invasive neck surgery have led to greater demands from imaging. Imaging needs to confidently localize the adenoma to a side, localize the adenoma to a quadrant or precise anatomic location, characterize the embry-

Received May 20, 2018; accepted after revision October 14.

From the Departments of Diagnostic Radiology (T.H.V., D.S., N.G.-T.), Biostatistics (J.S., W.W.), Imaging Physics (S.C.K.), Surgical Oncology (N.P.), and Nuclear Medicine (H.H.C., F.C.W.), The University of Texas MD Anderson Cancer Center, Houston, Texas; Department of Radiological Sciences (E.E.K.), University of California at Irvine, Orange, California; and Baylor College of Medicine (E.R.), Houston, Texas.

Thin H. Vu and Dawid Schellingerhout contributed equally to this work.

Please address correspondence to Thin H. Vu, MD, Department of Diagnostic Imaging, Unit 1482, The University of Texas MD Anderson Cancer Center, 1400 Pressler St, FCT 16.5036, Houston, TX 77030; e-mail: thinh.vu@mdanderson.org

<http://dx.doi.org/10.3174/ajnr.A5901>

logic origin of the parathyroid lesion, be sensitive to ectopic disease, and preferably be able to identify potential multigland disease. Some traditional imaging studies may not meet these modern requirements.

The purpose of the present study was to do a blinded comparison of the localizing capability of MIBI SPECT, 4DCT, and the combination of these 2 modalities using surgical localization as a criterion standard. We evaluated the ability of each technique to localize a parathyroid adenoma to a side and a quadrant, with particular note of reader confidence in the imaging findings to direct surgery.

MATERIALS AND METHODS

Study Population

This was a retrospective study of consecutive patients who were diagnosed with primary hyperparathyroidism between November 2009 and March 2010. All patients had biochemically confirmed primary hyperparathyroidism (a serum calcium level of >10.4 mg/dL [2.6 mmol/L] and a serum parathyroid hormone level of >65 pg/mL [6.84 pmol/L]); underwent preoperative MIBI SPECT and 4DCT performed on same scanner; and had pathologic confirmation by resection of a single hypercellular parathyroid gland. Patients who had undergone a prior operation or had multigland resections were excluded. We obtained a waiver of consent from our institutional review board (MD Anderson Cancer Center, Houston, Texas) for this Health Insurance Portability and Accountability Act–compliant study.

Image Acquisition

MIBI SPECT. All patients underwent a dual-phase MIBI study after intravenous injection of 20–25 mCi (740–925 MBq) of technetium Tc99m methoxyisobutyl isonitrile. Anterior and posterior planar images of the head, neck, and thorax were acquired at 20 and 90 minutes, and SPECT was acquired at 30–60 minutes after intravenous injection of technetium Tc99m methoxyisobutyl isonitrile. Images were acquired using a high-resolution, low-energy, parallel-hole collimator and a large FOV, dual-headed gamma camera with a jointly mounted 16-slice CT scanner (Symbia T16; Siemens, Erlangen, Germany). SPECT was acquired for 128 frames over a full 360° arc at 22 seconds per frame on a noncircular orbit mapped to the body contour. The gamma camera photopeak window was centered at 140 keV with a 15% window and an adjacent 15% scatter window at lower energy. The mean count per frame was 196,000 with a range of 136,000–256,000. A noncontrast low-dose CT scan (130 kV[peak], 90 mAs, pitch = 1.2, CareDose4D, nominal volume CT dose index = 9.7 mGy) was obtained immediately after SPECT acquisition for attenuation correction. Image reconstruction was performed using 3D-ordered subset expectation maximization (OSEM) (Flash3D; Siemens) with 8 iterations and 16 subsets and a 5-mm Gaussian postreconstruction filter to yield a $128 \times 128 \times 128$ matrix with $4.8 \times 4.8 \times 4.8$ mm voxels. CT-based attenuation correction, energy-window–based scatter correction, and collimator resolution modeling were used during SPECT reconstructions.

4DCT. The 4DCT study was performed on the same table immediately after the MIBI SPECT study using a 16-row multidetector CT scanner of the SPECT system (Symbia T16; Siemens). Helical

scans were obtained at 220 mA and 130 kVp. The scans were obtained with 1.25-mm collimation, table speed of 13.75 mm/s, pitch of 1.375, and gantry rotation time of 1 second. Initially, unenhanced scans were obtained from the carina to the mandible. An 18-ga intravenous cannula placed in the antecubital vein was used to inject 120 mL of nonionic contrast material, ioversol (Optiray 320; Mallinckrodt, St. Louis, Missouri), at 4.0 mL/s with a power injector. Multiphase scanning was performed with the second, third, and fourth scans (programmed to the same collimation, table feed, and duration as the first scan), which were obtained at 25 (arterial), 55 (venous), and 85 (delay) seconds, respectively, after the beginning of the administration of contrast.

Surgical Localization

The criterion standard for final anatomic localization of the parathyroid adenoma was an operation, as recorded in the operative notes.

Imaging Performance Analysis

Retrospective image analysis was performed on PACS workstations in configurations used for routine clinical image interpretation by 2 independent and blinded teams of readers. For each patient in the cohort, the MIBI SPECT was read independently using noncontrast CT and MIBI SPECT data only by 2 experienced nuclear physicians (E.E.K. and H.H.C.). The 4DCT data were read using both nonenhanced and contrast-enhanced CT data, as independently reviewed by 2 experienced neuroradiologists (D.S. and N.G.-T.). The combined MIBI SPECT and 4DCT (MIBI SPECT + 4DCT) data (all imaging information) were reviewed by a reader team consisting of an experienced neuroradiologist (T.H.V.) and a nuclear physician (E.R.). The team interpreted de-identified image sets knowing only the diagnosis of hyperparathyroidism, and readers were asked to localize the parathyroid adenoma. The localization to side (left or right) and quadrant (relative to the midpoint of the thyroid as dividing the upper and lower quadrants) and the embryologic origin of the abnormal parathyroid gland (superior or inferior) were recorded, as well as surgical localization based on surgical anatomy (Fig 1).¹⁷ For each localization, reader confidence (certain, equivocal, or uncertain on a 3-point scale) was also recorded. The reader team had no knowledge of the imaging data outside their assigned area. The images were interpreted as a consensus reading without individual readings to measure interrater agreement.

After all imaging analysis was performed, 1 researcher (F.C.W.) consulted the surgical and pathologic records to determine adenoma localization, pathologic characteristics, and weight.

Statistical Analysis

Error matrices were constructed for overall true-versus-false localization for each of the readings (MIBI SPECT, 4DCT, and MIBI SPECT + 4DCT) against surgical localization. Error matrices were then constructed by level of confidence and analyzed similarly. A 95% confidence interval for accuracy was calculated using the Clopper-Pearson exact method. Diagnostic accuracy was compared among MIBI SPECT, 4DCT, and MIBI SPECT + 4DCT and determined by the McNemar test. All tests were 2-sided, and P values $\leq .05$ were considered statistically signifi-

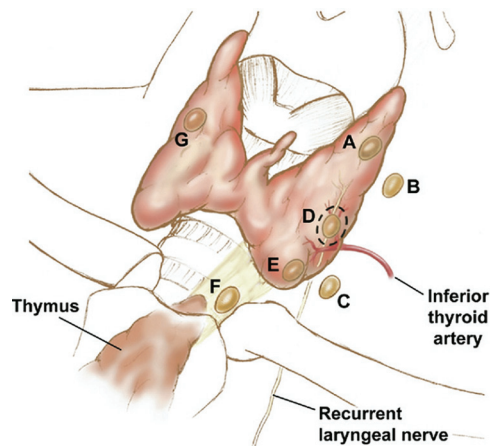


FIG 1. Surgical classification of parathyroid adenoma locations, anterior view. A, Superior, in proximity to the posterior surface of the thyroid parenchyma. B, Superior, fallen posteriorly into the tracheoesophageal groove and no longer in contact with the posterior surface of the thyroid tissue. C, Superior, fallen posteriorly into the tracheoesophageal groove and no longer in contact with the posterior surface of the thyroid tissue at the inferior pole close to the clavicles. D, Superior or inferior, in the midregion of the posterior surface of the thyroid parenchyma near the junction of the recurrent laryngeal nerve and the inferior thyroidal artery. E, Inferior, in the region inferior to the thyroid gland, lying in the anteroposterior plane of the thyroid and anterior to the trachea. F, Inferior, descended into the thyrothymic ligament or superior thymus and possibly appearing to be “ectopic” or in the mediastinum. G, Intrathyroidal.

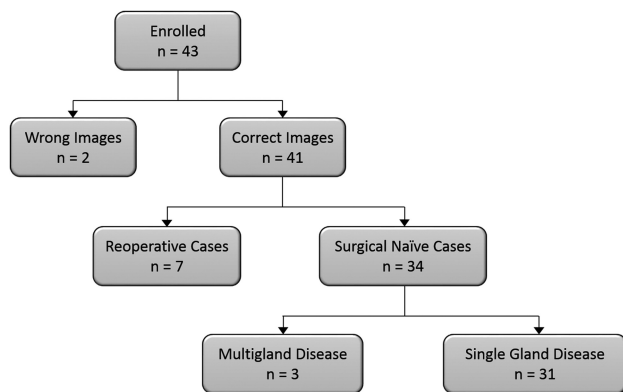


FIG 2. Patient selection flowchart. Thirty-one patients were included in the final analysis.

cant. Statistical analysis was performed using SAS, Version 9.4 (SAS Institute, Cary, North Carolina) and R version 2.3 (R Development Core Team, <http://www.r-project.org>).

RESULTS

Patient selection is summarized in Fig 2. Forty-three patients were included in our initial study group. Seven were excluded because of a prior operation, and 2 were excluded owing to incomplete imaging data, leaving 34 patients. Three patients had multiple parathyroid adenomas resected and were excluded. The remaining 31 patients had a single abnormal parathyroid gland resected.

The study group consisted of 6 male and 25 female patients with a median age of 56 years (range, 26–78 years). Patients had mean corrected calcium values of 10.6 mmol/L (median, 10.6 mmol/L; range, 9.5–11.8 mmol/L) against a reference range of 8.4–10.2 mmol/L at our laboratory. Patients had mean parathy-

Table 1: Diagnostic accuracy of left/right localization of parathyroid adenomas in the 31 patients in our study group

Imaging Modality	Left No. (%)	Right No. (%)	Total No. (%)	Accuracy (95% CI)
MIBI SPECT				93.5 (78.6–99.2)
Left	13 (41.9)	1 (3.2)	14 (45.2)	
Right	1 (3.2)	16 (51.6)	17 (54.8)	
4DCT				96.8 (83.3–99.9)
Left	14 (45.2)	1 (3.2)	15 (48.4)	
Right	0 (0.0)	16 (51.6)	16 (51.6)	
MIBI SPECT + 4DCT				96.8 (83.3–99.9)
Left	14 (45.2)	1 (3.2)	15 (48.4)	
Right	0 (0.0)	16 (51.6)	16 (51.6)	
Total	14 (45.2)	17 (54.8)		

Table 2: Diagnostic accuracy of embryologic origin of the abnormal parathyroid gland in the 31 patients in our study group

Imaging Modality	Superior No. (%)	Inferior No. (%)	Total No. (%)	Accuracy (95% CI)
MIBI SPECT				74.2 (55.4–88.1)
Superior gland	10 (32.3)	0 (0)	10 (32.3)	
Inferior gland	8 (25.8)	13 (41.9)	21 (67.7)	
Total	18 (58.1)	13 (41.9)		
4DCT				90.3 (74.3–98.0)
Superior gland	15 (48.4)	0 (0)	15 (48.6)	
Inferior gland	3 (9.7)	13 (41.9)	16 (51.6)	
Total	18 (58.1)	13 (41.9)		
MIBI SPECT + 4DCT				96.8 (83.3–99.9)
Superior gland	17 (54.8)	0 (0)	17 (54.8)	
Inferior gland	1 (3.2)	13 (41.9)	14 (45.2)	
Total	18 (58.1)	13 (41.9)		

roid hormone levels of 111 pmol/L (median, 105 pmol/L; range, 56–209 pmol/L) against a reference range of 9–80 pmol/L at our laboratory. The resected parathyroid glands had weights ranging from 0.07 to 6.08 g; the mean weight was 0.77 g and the median weight was 0.40 g.

Surgical Localization

Surgical resection localized parathyroid adenomas to the following locations: by side, 14 left and 17 right; by quadrant, 2 left inferior, 12 left superior, 11 right inferior, and 6 right superior; and by surgical classification (Fig 1), 9 type A, 9 type B, 3 type C, 1 type D, and 9 type E.

Overall Imaging Performance

Tables 1–4 summarize the error matrices for left- or right-sided localization, embryologic origin of the abnormal parathyroid gland (superior or inferior), quadrant localization (both left or right and upper or lower), and surgical classification of MIBI SPECT, 4DCT, and MIBI SPECT + 4DCT readings, along with accuracies.

MIBI SPECT achieved an accuracy of 93.5% (29 of 31 patients) in correctly localizing the parathyroid adenomas on the left or right side. Embryologic origin accuracy was 74.2% (23 of 31 patients). Quadrant localization accuracy was 67.7% (21 of 31 patients). Surgical classification accuracy was 54.8% (17 of 31 patients).

4DCT achieved an accuracy of 96.8% (30 of 31 patients) in correctly localizing parathyroid adenomas on the left or right side.

Table 3: Diagnostic accuracy of quadrant localization of parathyroid adenomas in the 31 patients in our study group

Imaging Modality	LI No. (%)	LS No. (%)	RI No. (%)	RS No. (%)	Total No. (%)	Accuracy (95% CI)
MIBI SPECT						67.7 (48.6–83.3)
LI	2 (6.5)	2 (6.5)	1 (3.2)	0 (0)	5 (16.1)	
LS	0 (0)	9 (29.0)	0 (0)	0 (0)	9 (29.0)	
RI	0 (0)	0 (0)	10 (32.3)	6 (19.4)	16 (51.6)	
RS	0 (0)	1 (3.2)	0 (0)	0 (0)	1 (3.2)	
4DCT						87.1 (70.2–96.4)
LI	2 (6.5)	1 (3.2)	1 (3.2)	0 (0)	4 (12.9)	
LS	0 (0)	11 (35.5)	0 (0)	0 (0)	11 (35.5)	
RI	0 (0)	0 (0)	10 (32.3)	2 (6.5)	12 (38.7)	
RS	0 (0)	0 (0)	0 (0)	4 (12.9)	4 (12.9)	
MIBI SPECT + 4DCT						93.5 (78.6–99.2)
LI	2 (6.5)	0 (0)	1 (3.2)	0 (0)	3 (9.7)	
LS	0 (0)	12 (38.7)	0 (0)	0 (0)	12 (38.7)	
RI	0 (0)	0 (0)	10 (32.3)	1 (3.2)	11 (35.5)	
RS	0 (0)	0 (0)	0 (0)	5 (16.1)	5 (16.1)	
Total	2 (6.5)	12 (38.7)	11 (35.5)	6 (19.4)		

Note:—LI indicates left inferior; LS, left superior; RI, right inferior; RS, right superior.

Table 4: Diagnostic accuracy of surgical classification (Fig 1) of parathyroid adenomas in the 31 patients in our study group

Imaging Modality	A No. (%)	B No. (%)	C No. (%)	D No. (%)	E No. (%)	Total No. (%)	Accuracy (95% CI)
MIBI SPECT							54.8 (36.0–72.7)
A	3 (9.7)	1 (3.2)	0 (0)	0 (0)	0 (0)	4 (12.9)	
B	2 (6.5)	3 (9.7)	0 (0)	0 (0)	0 (0)	5 (16.1)	
C	2 (6.5)	2 (6.5)	3 (9.7)	1 (3.2)	0 (0)	8 (25.8)	
D	0 (0)	1 (3.2)	0 (0)	0 (0)	0 (0)	1 (3.2)	
E	2 (6.5)	2 (6.5)	0 (0)	0 (0)	8 (25.8)	12 (38.7)	
F	0 (0)	0 (0)	0 (0)	0 (0)	1 (3.2)	1 (3.2)	
4DCT							61.3 (42.2–78.2)
A	7 (22.6)	4 (12.9)	0 (0)	0 (0)	0 (0)	11 (35.5)	
B	1 (3.2)	2 (6.5)	0 (0)	0 (0)	0 (0)	3 (9.7)	
C	0 (0)	1 (3.2)	3 (9.7)	0 (0)	0 (0)	4 (12.9)	
D	0 (0)	0 (0)	0 (0)	1 (3.2)	3 (9.7)	4 (12.9)	
E	1 (3.2)	2 (6.5)	0 (0)	0 (0)	6 (19.4)	9 (29.0)	
F	0 (0)	0 (0)	0 (0)	0 (0)	0 (0)	0 (0)	
MIBI SPECT + 4DCT							74.2 (55.4–88.1)
A	7 (22.6)	3 (9.7)	0 (0)	0 (0)	0 (0)	10 (32.3)	
B	0 (0)	4 (12.9)	0 (0)	0 (0)	0 (0)	4 (12.9)	
C	0 (0)	2 (6.5)	3 (9.7)	1 (3.2)	0 (0)	6 (19.4)	
D	2 (6.5)	0 (0)	0 (0)	0 (0)	0 (0)	2 (6.5)	
E	0 (0)	0 (0)	0 (0)	0 (0)	9 (29)	9 (29.0)	
F	0 (0)	0 (0)	0 (0)	0 (0)	0 (0)	0 (0)	
Total	9 (29)	9 (29)	3 (9.7)	1 (3.2)	9 (29.0)		

Embryologic origin accuracy was 90.3% (28 of 31 patients). Quadrant localization accuracy was 87.1% (27 of 31 patients). Surgical classification accuracy was 61.3% (19 of 31 patients).

MIBI SPECT + 4DCT achieved an accuracy of 96.8% (30 of 31 patients) in correctly localizing the parathyroid adenomas on the left or right side. Embryologic origin accuracy was 96.8% (30 of 31 patients). Quadrant localization accuracy was 93.5% (29 of 31 patients). Surgical classification accuracy was 74.2% (23 of 31 patients).

We found that most errors in MIBI SPECT were due to superior glands being misidentified as inferior glands (Table 2), whereas this error was much less frequently observed in the 4DCT and MIBI SPECT + 4DCT readings.

Imaging Performance by Confidence Level

Table 5 shows reader team confidence in each localization technique. Confidence levels were generally higher for 4DCT and MIBI SPECT + 4DCT readings than they were for MIBI SPECT readings. Confidence in left/right localization was generally much

Table 5: Level of confidence response from 3 reading groups for lateralization, upper/lower quadrant localization, and localization by surgical classification

Response/Imaging Modality	Certain (%)	Equivocal (%)	Uncertain (%)
Lateralization			
MIBI SPECT	27 (87.1)	1 (3.2)	3 (9.7)
4DCT	30 (96.8)	1 (3.2)	0 (0.0)
MIBI SPECT + 4DCT	29 (93.5)	2 (6.5)	0 (0.0)
Upper/lower			
MIBI SPECT	22 (71.0)	6 (19.4)	3 (9.7)
4DCT	30 (96.8)	1 (3.2)	0 (0.0)
MIBI SPECT + 4DCT	31 (100.0)	0 (0.0)	0 (0.0)
Surgical localization			
MIBI SPECT	15 (48.4)	15 (48.4)	1 (3.2)
4DCT	28 (90.3)	3 (9.7)	0 (0.0)
MIBI SPECT + 4DCT	29 (93.5)	1 (3.2)	1 (3.2)

higher than for quadrant localization. The more detailed level of surgical classification reduced confidence levels for MIBI SPECT to a greater degree than it did for 4DCT and MIBI SPECT +

Table 6: McNemar test of paired imaging modalities for diagnostic accuracy of left/right localization of parathyroid adenomas in the 31 patients in our study group

Imaging Modality	Correct	Wrong	Total	P Value
4DCT vs				
MIBI SPECT				
Correct	28	1	29	.56
Wrong	2	0	2	
Total	30	1	31	
MIBI SPECT + 4DCT vs				
4DCT				
Correct	29	1	30	1.00
Wrong	1	0	1	
Total	30	1	31	
MIBI SPECT + 4DCT vs				
MIBI SPECT				
Correct	28	1	29	.56
Wrong	2	0	2	
Total	30	1	31	

Table 7: McNemar test of paired imaging modalities for diagnostic accuracy of embryologic origin of the abnormal parathyroid gland in the 31 patients in our study group

Imaging Modality	Correct	Wrong	Total	P Value
4DCT vs				
MIBI SPECT				
Correct	22	1	23	.06
Wrong	6	2	8	
Total	28	3	31	
MIBI SPECT + 4DCT vs				
4DCT				
Correct	28	0	28	.16
Wrong	2	1	3	
Total	30	1	31	
MIBI SPECT + 4DCT vs				
MIBI SPECT				
Correct	23	0	23	.008
Wrong	7	1	8	
Total	30	1	31	

Table 8: McNemar test of paired imaging modalities for diagnostic accuracy of quadrant localization of the abnormal parathyroid gland in the 31 patients in our study group

Imaging Modality	Correct	Wrong	Total	P Value
4DCT vs				
MIBI SPECT				
Correct	19	2	21	.06
Wrong	8	2	10	
Total	27	4	31	
MIBI SPECT + 4DCT vs				
4DCT				
Correct	26	1	27	.32
Wrong	3	1	4	
Total	29	2	31	
MIBI SPECT + 4DCT vs				
MIBI SPECT				
Correct	20	1	21	.01
Wrong	9	1	10	
Total	29	2	31	

4DCT, for which confidence was fairly consistently high regardless of the level of detail required.

Comparison of Imaging Modalities

Tables 6-9 summarize McNemar test results comparing the diagnostic accuracy of left- or right-sided localization, embryologic origin of the abnormal parathyroid gland (superior or inferior),

Table 9: McNemar test of paired imaging modalities for diagnostic accuracy of surgical localization of the abnormal parathyroid gland in the 31 patients in our study group

Imaging Modality	Correct	Wrong	Total	P Value
4DCT vs				
MIBI SPECT				
Correct	11	6	17	.06
Wrong	8	6	14	
Total	19	12	31	
MIBI SPECT + 4DCT vs				
4DCT				
Correct	16	3	19	0.21
Wrong	7	5	12	
Total	23	8	31	
MIBI SPECT + 4DCT vs				
MIBI SPECT				
Correct	15	2	17	.06
Wrong	8	6	14	
Total	23	8	31	

quadrant localization (both left/right and upper/lower), and surgical classification among MIBI SPECT, 4DCT, and MIBI SPECT + 4DCT.

McNemar test results comparing the diagnostic accuracy of left- or right-sided localization revealed no statistically significant differences, indicating substantially similar diagnostic performance.

McNemar test results comparing the diagnostic accuracy of embryologic origin revealed that MIBI SPECT + 4DCT was significantly better than MIBI SPECT ($P = .008$) and 4DCT was better than MIBI SPECT on the borderline of statistical significance ($P = .06$).

McNemar test results comparing the diagnostic accuracy of quadrant localization revealed that MIBI SPECT + 4DCT was significantly better than MIBI SPECT ($P = .01$) and 4DCT was better than MIBI SPECT on the borderline of statistical significance ($P = .06$).

McNemar test results comparing the diagnostic accuracy of surgical localization revealed that MIBI SPECT + 4DCT was better than MIBI SPECT on the borderline of statistical significance ($P = .06$).

Examples of correct and incorrect localization are shown in Figs 3 and 4. Figure 3 shows a large right tracheoesophageal groove parathyroid adenoma that was correctly localized by 3 modalities. Figure 4 shows a small left paraesophageal parathyroid adenoma that had correct left/right and quadrant localization by 4DCT and MIBI SPECT + 4DCT and correct left/right localization and incorrect quadrant localization by MIBI SPECT.

DISCUSSION

Our results showed that overall, MIBI SPECT was less accurate than 4DCT, which, in turn, was less accurate than combined MIBI SPECT + 4DCT. All imaging methods performed equally well in correctly localizing the parathyroid adenoma to the left or right side, and most of the inconsistency between MIBI SPECT and 4DCT was a result of errors in classification of embryologic origin. MIBI SPECT + 4DCT showed clear superiority over MIBI SPECT for embryologic and quadrant localization. Although our results were only marginally statistically significant, 4DCT may be better than MIBI SPECT for embryologic and quadrant localization and

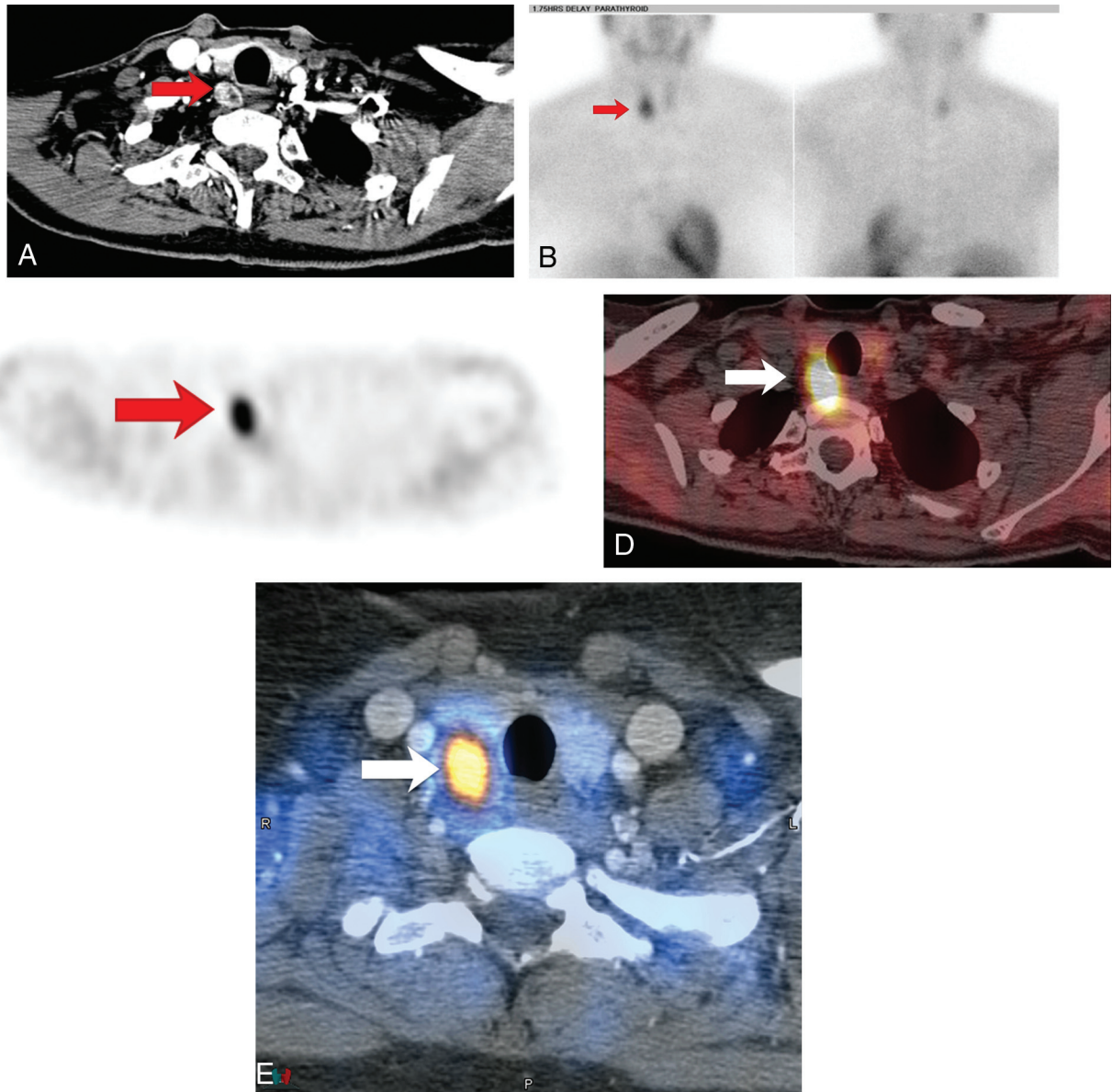


FIG 3. A, The axial arterial phase of a multiphase multidetector 4D CT image shows a right tracheoesophageal parathyroid adenoma (type C; Fig 1). B, Anterior and posterior delay planar scintigraphy shows retention of the radiotracer on the right side. C, An axial SPECT image shows retention of the radiotracer in the lower neck. D, An axial SPECT image fused to a noncontrast CT image localizes the retention of the radiotracer to the right tracheoesophageal groove. E, An axial SPECT image fused to the axial arterial phase of a multiphase multidetector 4D CT image localizes the retention of the radiotracer with concomitant early enhancement to the right tracheoesophageal groove. Red and white arrows show the parathyroid adenoma.

MIBI SPECT + 4DCT may be better than MIBI SPECT for surgical localization. The confidence of readers' localizations was generally higher with 4DCT and MIBI SPECT + 4DCT than it was with MIBI SPECT. The differential in both imaging performance and reader confidence decreased as the required level of detail in anatomic localization increased.

A recent meta-analysis of 24 published MIBI SPECT studies evaluating 1276 patients, in which patients with mixed diagnoses, secondary hyperparathyroidism, previous surgeries, and multigland disease were excluded, showed that MIBI SPECT had an estimated pooled sensitivity of 86%.¹⁸ In a recent retrospective study of 65 patients with primary hyperparathyroidism, MIBI SPECT accurately localized the offending parathyroid gland with an average weight of 0.82 g in 80% of cases.¹⁹ Compared with

these previous studies, our study showed improved accuracy of MIBI SPECT for left/right localization and diminished accuracy of MIBI SPECT for quadrant localization. This could be explained by the poor image resolution of SPECT and lack of anatomic detail in low-dose CT for discriminating parathyroid adenomas from the thyroid gland. The ability to make this distinction would aid in quadrant localization of the adenoma as well as surgical classification.

Several investigators have shown that low-dose CT added to SPECT or MIBI SPECT can improve the diagnostic value for accurate localization of parathyroid adenomas.^{12,20} Our study showed a substantial improvement in parathyroid adenoma localization accuracy with MIBI SPECT + 4DCT, or "diagnostic CT" added to SPECT, compared with MIBI SPECT alone.

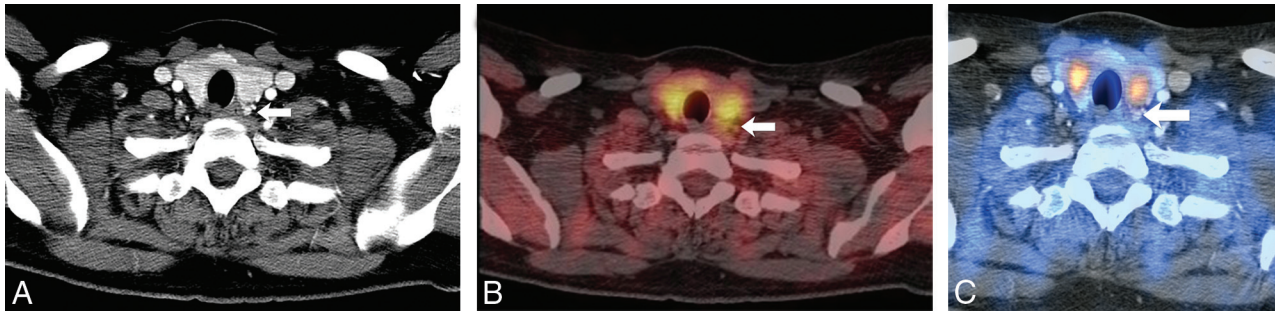


FIG 4. A case in which 4DCT could diagnose a parathyroid adenoma in the face of a sestamibi study with negative findings. *A*, The axial arterial phase of a multiphase multidetector 4D CT image shows a small early-enhancing left paraesophageal parathyroid adenoma (*arrow*). *B*, An axial MIBI SPECT image fused to a noncontrast CT image reveals no retention of the radiotracer in the left central compartment of a surgically proven parathyroid adenoma, which was effectively demonstrated on 4DCT (*arrow*). *C*, An axial SPECT image fused to the axial arterial phase of a multiphase multidetector 4D CT image shows a small early-enhancing left paraesophageal parathyroid adenoma (*arrow*).

In a retrospective study of 143 patients with primary hyperparathyroidism and no previous neck surgery, 4DCT had a sensitivity of 93.7% for left/right localization and 86.6% for quadrant localization.¹⁵ Compared with that study, we report slightly improved accuracy of 4DCT for left/right localization and similar accuracy for quadrant localization. A recent meta-analysis of thirty-four 4DCT studies evaluating 2563 patients showed a pooled sensitivity of 81% for left/right localization and 73% for quadrant localization.²¹ Compared with that study, we report improved accuracy of 4DCT for left/right localization and quadrant localization. This may be because our 4DCT imaging protocol used 4 phases, similar to the protocol described by Hunter et al,¹⁵ whereas the meta-analysis represented various CT protocols across studies, ranging from 1 to 4 phases. In addition, the meta-analysis included studies of patients with previous operations and multigland disease, which, in our experience, are likely to be harder to interpret.

Heiba et al²² compared neck pinhole dual-tracer and dual-phase sestamibi with and without SPECT for localization of 153 parathyroid adenomas, and they found that pinhole dual-tracer SPECT had significantly higher sensitivity (93%) than dual-phase SPECT (68%), SPECT with only pinhole delay (39%), pinhole dual-tracer CT alone (25%), and dual-phase CT alone (18%). In a prospective study comparing dual-isotope subtraction pinhole scintigraphy, dual-phase SPECT, 4DCT, and sonography in 91 patients with 97 parathyroid adenomas, Krakauer et al²³ found that the sensitivity of dual-isotope subtraction pinhole scintigraphy was 93%. The sensitivity of dual-phase SPECT (65%), 4DCT (58%), and sonography (57%) was significantly lower. In our study, we confirmed that dual-phase MIBI SPECT has lower localization accuracy compared with dual-isotope subtraction scintigraphy. In our study, 4DCT and MIBI SPECT + 4DCT yielded a sensitivity similar to that of dual-isotope subtraction scintigraphy.

The use of combined CT imaging modalities raises concerns about radiation exposure. The mean effective dose for 22.5 mCi of sestamibi is estimated at 7.5 mSv. The mean effective dose for 4DCT is 17.9 mSv (volume CT dose index = 20.8 mGy). Our effective dose for sestamibi was 7.5 mSv, and our dose with 4DCT was 17.9 mSv. These doses are similar to those in a recent article evaluating the total effective radiation doses associated with 4DCT (20.2 ± 2.8 mSv) and sestamibi (5.6 ± 0.24 mSv) used for parathyroid adenoma localization before surgery.²⁴ The total ef-

fective dose of MIBI SPECT + 4DCT is estimated at 27.7 mSv, which includes contributions from the low-dose noncontrast CT for SPECT attenuation correction. Although there are no good data on cancer incidence after low radiation exposure, conservatively, the net radiation exposure increases a patient's annual cancer risk by 0.019% and lifetime cancer risk by 0.52% compared with the baseline cancer incidence.^{25,26} We believe that this is a favorable risk/benefit ratio given the very small cancer risk balanced against the serious health consequences of persistent hyperparathyroidism, especially in an older patient population.

The main strength of our study is the fully blinded, unbiased evaluation of different imaging modalities, all of which were acquired and viewed on identical platforms, thus eliminating any concerns about image coregistration or image interpretation in different environments. We also used a highly reliable reference standard and defined the exact location of each lesion by cross-referencing the histopathology reports and the operating notes with the imaging studies. In addition, all imaging scans were reviewed by expert radiologists or nuclear medicine physicians with considerable clinical experience in the interpretation of parathyroid localization studies. We directly compared MIBI SPECT and 4DCT as well as MIBI SPECT with diagnostic 4DCT to evaluate the incremental diagnostic value for parathyroid adenoma detection.

Limitations of this study include its retrospective nature and the small sample size. We included only patients with single-gland disease because of the limited sample size of multigland disease and the considerable differences between single- and multigland disease both biologically and in image interpretation. None of our imaging tests could perfectly localize lesions in the surgical classification scheme by Perrier et al,¹⁷ but this classification is based on features (such as the location of the recurrent laryngeal nerve) that cannot yet be perceived by imaging and is thus of greater utility in the intraoperative environment.

CONCLUSIONS

Our results suggest that although all imaging modalities are useful for localizing parathyroid adenomas, MIBI SPECT + 4DCT is superior and 4DCT is marginally better than MIBI SPECT for determining embryologic and quadrant-level localization, particularly when detailed anatomic information is required, such as that needed to direct minimally invasive (targeted) surgery. This finding may strengthen the role of MIBI SPECT + 4DCT and

4DCT as first-line imaging techniques for preoperative localization. The confidence observed in localization, particularly useful to surgeons who need actionable information to plan minimally invasive surgery, was also higher for 4DCT than for MIBI SPECT. Combined interpretation of MIBI SPECT + 4DCT showed a still further increase in diagnostic accuracy and confidence beyond 4DCT alone, suggesting that 4DCT and MIBI SPECT are complementary modalities, supplying nonoverlapping information that might be useful, especially in difficult diagnostic cases.

ACKNOWLEDGMENTS

The authors thank Erica Goodoff for her assistance in editing.

Disclosures: W. Wei—UNRELATED: Grant: National Institutes of Health/National Cancer Institute, Comments: P30 CA016672.* S. Cheenu Kappadath—UNRELATED: Consultancy: BTG International Inc; Grants: GE Healthcare, BTG International Inc.* Hubert H. Chuang—UNRELATED: Consultancy: SAGE Consulting. *Money paid to the institution.

REFERENCES

- Rosen CJ; American Society for Bone and Mineral Research. *Primer on the Metabolic Bone Diseases and Disorders of Mineral Metabolism*. Ames: Wiley-Blackwell; 2013
- Mihai R, Barczynski M, Iacobone M, et al. **Surgical strategy for sporadic primary hyperparathyroidism an evidence-based approach to surgical strategy, patient selection, surgical access, and reoperations.** *Langenbecks Arch Surg* 2009;394:785–98 CrossRef Medline
- Thomas DL, Bartel T, Menda Y, et al. **Single photon emission computed tomography (SPECT) should be routinely performed for the detection of parathyroid abnormalities utilizing technetium-99m sestamibi parathyroid scintigraphy.** *Clin Nucl Med* 2009;34:651–55 CrossRef Medline
- Lindqvist V, Jacobsson H, Chandanos E, et al. **Preoperative 99Tc(m)-sestamibi scintigraphy with SPECT localizes most pathologic parathyroid glands.** *Langenbecks Arch Surg* 2009;394:811–15 CrossRef Medline
- Smith RB, Evasovich M, Girod DA, et al. **Ultrasound for localization in primary hyperparathyroidism.** *Otolaryngol Head Neck Surg* 2013; 149:366–71 CrossRef Medline
- Levy JM, Kandil E, Yau LC, et al. **Can ultrasound be used as the primary screening modality for the localization of parathyroid disease prior to surgery for primary hyperparathyroidism? A review of 440 cases.** *ORL J Otorhinolaryngol Relat Spec* 2011;73:116–20 CrossRef Medline
- Rodgers SE, Hunter GJ, Hamberg LM, et al. **Improved preoperative planning for directed parathyroidectomy with 4-dimensional computed tomography.** *Surgery* 2006;140:932–40; discussion 940–41 CrossRef Medline
- Kabala JE. **Computed tomography and magnetic resonance imaging in diseases of the thyroid and parathyroid.** *Eur J Radiol* 2008;66: 480–92 CrossRef Medline
- Weber T, Maier-Funk C, Ohlhauser D, et al. **Accurate preoperative localization of parathyroid adenomas with C-11 methionine PET/CT.** *Ann Surg* 2013;257:1124–28 CrossRef Medline
- Orevi M, Freedman N, Mishani E, et al. **Localization of parathyroid adenoma by ¹¹C-choline PET/CT: preliminary results.** *Clin Nucl Med* 2014;39:1033–38 CrossRef Medline
- Krausz Y, Bettman L, Guralnik L, et al. **Technetium-99m-MIBI SPECT/CT in primary hyperparathyroidism.** *World J Surg* 2006;30: 76–83 CrossRef Medline
- Lavelly WC, Goetze S, Friedman KP, et al. **Comparison of SPECT/CT, SPECT, and planar imaging with single- and dual-phase (99m)Tc-sestamibi parathyroid scintigraphy.** *J Nucl Med* 2007;48:1084–89 CrossRef Medline
- Vaz A, Griffiths M. **Parathyroid imaging and localization using SPECT/CT: initial results.** *J Nucl Med Technol* 2011;39:195–200 CrossRef Medline
- Starker LF, Mahajan A, Björklund P, et al. **4D parathyroid CT as the initial localization study for patients with de novo primary hyperparathyroidism.** *Ann Surg Oncol* 2011;18:1723–28 CrossRef Medline
- Hunter GJ, Schellingerhout D, Vu TH, et al. **Accuracy of four-dimensional CT for the localization of abnormal parathyroid glands in patients with primary hyperparathyroidism.** *Radiology* 2012;264: 789–95 CrossRef Medline
- Kelly HR, Hamberg LM, Hunter GJ. **4D-CT for preoperative localization of abnormal parathyroid glands in patients with hyperparathyroidism: accuracy and ability to stratify patients by unilateral versus bilateral disease in surgery-naive and re-exploration patients.** *AJNR Am J Neuroradiol* 2014;35:176–81 CrossRef Medline
- Perrier ND, Edeiken B, Nunez R, et al. **A novel nomenclature to classify parathyroid adenomas.** *World J Surg* 2009;33:412–16 CrossRef Medline
- Wong KK, Fig LM, Gross MD, et al. **Parathyroid adenoma localization with 99mTc-sestamibi SPECT/CT: a meta-analysis.** *Nucl Med Commun* 2015;36:363–75 CrossRef Medline
- Keidar Z, Solomonov E, Karry R, et al. **Preoperative [99mTc]MIBI SPECT/CT interpretation criteria for localization of parathyroid adenomas: correlation with surgical findings.** *Mol Imaging Biol* 2017;19:265–70 CrossRef Medline
- Neumann DR, Obuchowski NA, Difilippo FP. **Preoperative 123I/99mTc-sestamibi subtraction SPECT and SPECT/CT in primary hyperparathyroidism.** *J Nucl Med* 2008;49:2012–17 CrossRef Medline
- Kluijfhout WP, Pasternak JD, Beninato T, et al. **Diagnostic performance of computed tomography for parathyroid adenoma localization: a systematic review and meta-analysis.** *Eur J Radiol* 2017;88:117–28 CrossRef Medline
- Heiba SI, Jiang M, Rivera J, et al. **Direct comparison of neck pinhole dual-tracer and dual-phase MIBI accuracies with and without SPECT/CT for parathyroid adenoma detection and localization.** *Clin Nucl Med* 2015;40:476–82 CrossRef Medline
- Krakauer M, Wieslander B, Myschetzky PS, et al. **A prospective comparative study of parathyroid dual-phase scintigraphy, dual-isotope subtraction scintigraphy, 4D-CT, and ultrasonography in primary hyperparathyroidism.** *Clin Nucl Med* 2016;41:93–100 CrossRef Medline
- Moosvi SR, Smith S, Hathorn J, et al. **Evaluation of the radiation dose exposure and associated cancer risks in patients having preoperative parathyroid localization.** *Ann R Coll Surg Engl* 2017;99: 363–68 CrossRef Medline
- Ray P, Vu T, Romero M, et al. **Limiting the risks of radiation exposure in diagnostic imaging.** *Surgery* 2014;156:1297–99 CrossRef Medline
- Hoang JK, Reiman RE, Nguyen GB, et al. **Lifetime attributable risk of cancer from radiation exposure during parathyroid imaging: comparison of 4D CT and parathyroid scintigraphy.** *AJR Am J Roentgenol* 2015;204:W579–85 CrossRef Medline